

# Grounding the Score: Explicit Visual Premise Verification for Reliable VLM Process Reward Models

Junxin Wang<sup>\*1,2</sup>, Dai Guan<sup>\*1</sup>, Weijie Qiu<sup>3</sup>, Zhihang Li<sup>\*1</sup>, Yongbo Gai<sup>1</sup>, Zhengyi Yang<sup>2</sup>, Mengyu Zhou<sup>1</sup>, Erchao Zhao<sup>1</sup>, Xiaoxi Jiang<sup>1</sup> and Guanjun Jiang<sup>1</sup>

<sup>1</sup>Qwen Large Model Application Team, Alibaba, <sup>2</sup>Institute of Automation, Chinese Academy of Sciences, <sup>3</sup>Beijing University of Posts and Telecommunications

\*Equal contribution. \*Work done during an internship at Alibaba. †Corresponding author.

Vision-language process reward models (VL-PRMs) are increasingly used to score intermediate reasoning steps and rerank candidates under test-time scaling, yet they often function as black-box judges: a low step score may reflect a genuine reasoning mistake or simply the verifier’s own misperception of the image. This entanglement between perception and reasoning leads to systematic false positives (rewarding hallucinated visual premises) and false negatives (penalizing correct grounded statements), undermining both reranking and error localization. We introduce **Explicit Visual Premise Verification (EVPV)**, a lightweight verification interface that conditions step scoring on the reliability of the visual premises a step depends on. Specifically, the policy is prompted to produce a step-wise *visual checklist* that makes its required visual facts explicit, while a constraint extractor independently derives *structured visual constraints* from the input image. EVPV matches checklist claims against these constraints to compute a scalar *visual reliability* signal, and calibrates PRM step rewards via reliability gating: rewards for visually dependent steps are attenuated when reliability is low and preserved when reliability is high, decoupling perceptual uncertainty from logical evaluation without per-step tool calls. Experiments on VisualProcessBench and six multimodal reasoning benchmarks show that EVPV improves step-level verification and consistently boosts Best-of- $N$  reranking accuracy over strong baselines. Furthermore, injecting controlled corruption into the extracted constraints produces monotonic performance degradation, providing causal evidence that the gains arise from constraint fidelity and explicit premise verification rather than incidental prompt effects. The relevant code has been open-sourced at <https://github.com/Qwen-Applications/EVPV-PRM>.

## 1. Introduction

Multimodal mathematical reasoning requires models to jointly solve two tightly coupled but failure-prone subproblems: *visual perception* (reading diagrams, extracting quantities from tables, OCR, and geometric relations) and *symbolic reasoning* (logical derivation and computation). While contemporary multimodal LLMs can produce fluent multi-step solutions, their correctness is frequently bottlenecked by grounding: a single perceptual mistake may redirect the entire derivation while keeping later steps locally coherent. This makes *process-level* verification and selection—not only final-answer checking—central to robust deployment, especially under test-time scaling regimes such as Best-of- $N$  and search-based decoding (Zheng et al., 2025; Ma et al., 2023; Zhang et al., 2024a).

Process reward models (PRMs) operationalize process supervision by assigning step-wise scores to reasoning traces, and they are widely used for Best-of- $N$  reranking, guided search, and post-training (Zheng et al., 2025; Ma et al., 2023; Zhang et al., 2024a). In the vision-language setting, dedicated PRMs and benchmarks such as VisualPRM and VisualProcessBench have shown that step-aware critics can improve multimodal reasoning under test-time scaling (Wang et al., 2025b), and data-efficient recipes further lower the cost of training such verifiers (Wang et al., 2025a). These advances have been instrumental in unlocking the latent capability of

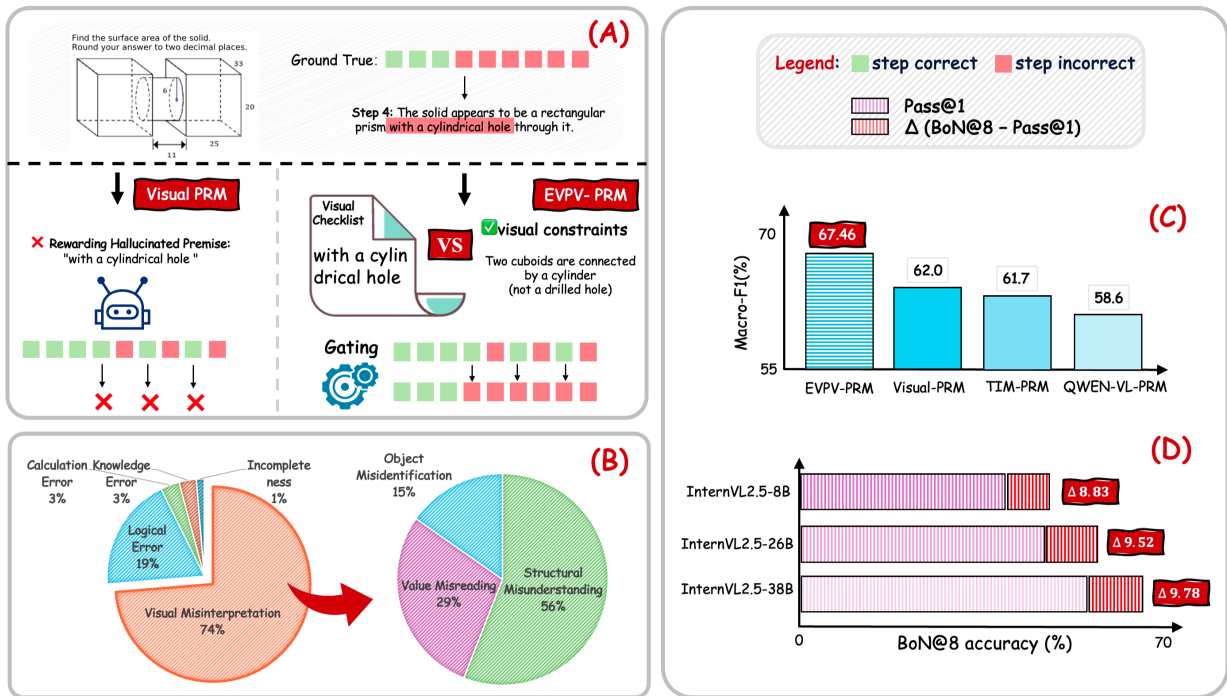


Figure 1 | **EVPV: premise-aware process reward modeling for reliable multimodal reasoning.** (A) *Motivating failure case.* A standard VL-PRM (VisualPRM) can reward a locally fluent step that relies on a hallucinated visual premise (e.g., “a cylindrical hole”). EVPV prompts the policy to state an explicit visual checklist, verifies it against independently extracted structured visual constraints, and gates step rewards when the premise is unreliable. (B) *Where step errors come from.* On VisualProcessBench, most step errors stem from visual misinterpretation (left); these errors are dominated by structural misunderstandings and value misreadings (right), motivating explicit premise verification. (C) *Step-level verification.* EVPV-PRM achieves higher overall Macro-F1 on VisualProcessBench than prior multimodal PRMs. (D) *Deployable test-time gains.* Under Best-of-8 reranking for InternVL2.5 policies, EVPV-PRM yields consistent BoN@8 improvements  $\Delta = \text{BoN@8} - \text{Pass@1}$  across model scales, indicating more reliable selection of grounded solutions under test-time scaling.

strong open multimodal policies (Zhu et al., 2025). Yet, when deployed in the wild, current vision-language PRMs still behave like *black-box judges*: a low score on a step is hard to interpret—did the step fail logically, or did the verifier itself misperceive the image? Similar reliability concerns—e.g., overconfidence and uncertainty miscalibration in step-wise judgments—have also been noted for PRMs more broadly (Ye et al., 2025; Park et al., 2025).

This ambiguity is not merely a diagnostic inconvenience; it is a systematic source of verification error. If the PRM’s own visual grounding is unreliable, it can assign low scores to correct visual descriptions (*false negatives*) or high scores to hallucinated ones (*false positives*), undermining both reranking and error localization. Figure 1 illustrates this failure mode: VisualPRM rewards a locally fluent step that assumes a nonexistent “cylindrical hole,” whereas EVPV makes the visual premise explicit, verifies it against structured visual constraints, and gates the step reward when the premise is not supported. The error breakdown in Figure 1 further shows that visual misinterpretation dominates step errors on VisualProcessBench (Wang et al., 2025b). More generally, recent audits have shown that PRM signals can be sensitive to semantic perturbations and may reward fluent but unsupported content under distribution shift (Cheng et al., 2025; Ye et al., 2025).

These observations motivate our core hypothesis: *perceptual correctness is a prerequisite for meaningful logical evaluation.* A step that is built on an incorrect visual premise is wrong regardless of how impeccable the subsequent algebra may be. Consequently, a verifier that directly predicts step correctness without explicitly validating the underlying visual premise is forced to entangle two error sources—perception and reasoning—and will remain brittle under early catastrophic misreads. Tool-integrated verification offers one principled path by independently querying the image to reduce confirmation bias (Kuang et al., 2025), but step-wise tool calls can

be prohibitively expensive when scoring long traces at Best-of- $N$  scale (Ma et al., 2023; Zhang et al., 2024a).

We therefore introduce *Explicit Visual Premise Verification (EVPV)* as a lightweight mechanism that makes a PRM “qualified” to judge reasoning steps. The policy is prompted to provide a *visual checklist*—explicit visual premises that each step relies on. In parallel, we extract structured visual facts from the image into a constraint set (numeric readings, geometric relations, and compositional structure). EVPV first verifies whether the checklist is supported by these visual facts, producing a reliability signal; only when the visual premise is deemed reliable do we enforce strict logical scoring. Concretely, we calibrate step rewards by gating visually dependent steps with the estimated visual reliability, attenuating rewards toward neutrality when the premise is unreliable and preserving them when it is well supported. This decouples visual understanding from step judgment, reduces false positives/negatives caused by verifier-side misperception, and yields more stable reranking gains. As previewed in Figure 1 (C), this premise-aware calibration improves step-level verification performance on VisualProcessBench.

We evaluate EVPV on VisualProcessBench and multiple multimodal reasoning benchmarks under Best-of- $N$  reranking. Our method achieves higher step-level verification performance and more deployable reranking improvements than strong multimodal PRM baselines (Wang et al., 2025b,a), while avoiding the heavy cost of step-wise tool invocation (Kuang et al., 2025). Figure 1 (D) further shows that these gains translate into consistent BoN@8 improvements across InternVL2.5 policy scales, indicating more reliable selection under test-time scaling. Moreover, controlled corruption of extracted constraints yields a monotonic performance degradation curve, supporting that the gains arise from improved visual premise verification rather than incidental prompt effects.

## 2. Related Work

**Process reward models.** Process reward models (PRMs) provide step-level supervision and have become a core mechanism for test-time scaling (e.g., Best-of- $N$  reranking), guided decoding, and post-training of reasoning models (Zheng et al., 2025; Ma et al., 2023; Zhang et al., 2024a). Beyond standard discriminative PRMs that directly score steps, recent work has explored verifiers that *think* before judging: R-PRM generates explicit analyses to improve step discrimination and stability (She et al., 2025), and GenPRM treats verification as a generative reasoning procedure that can itself be scaled at inference time (Zhao et al., 2025). Related reasoning-centric reward modeling further encourages explicit deliberation, including reward models that generate long-form rationales before producing preferences (Guo et al., 2025) and process reward models that think via generative verification (Khalifa et al., 2025; Jia et al., 2025). Other lines improve PRM learning objectives and usage: DG-PRM introduces dynamic, multi-criteria reward allocation and multi-objective optimization (Yin et al., 2025), ER-PRM proposes entropy-regularized process-value estimation to obtain more robust process signals (Zhang et al., 2024b), and BiPRM leverages bidirectional evaluation to incorporate future context when scoring earlier steps (Zhang et al., 2025d). Complementary work revisits the formulation of process values, e.g., learning Q-value rankings over steps (Li & Li, 2024), and addresses training-time pathologies such as reward hacking via alternative credit assignment (Cheng et al., 2025). Data and supervision pipelines have also been studied extensively: ACTPRM reduces labeling costs via uncertainty-driven active learning (Duan et al., 2025); AURORA automates PRM training via ensemble prompting and reverse verification (Tan et al., 2025); VersaPRM extends PRMs beyond math by leveraging synthetic multi-domain reasoning traces (Zeng et al., 2025); and OpenPRM constructs open-domain process-based reward models from preference trees distilled from outcome-level supervision (Zhang et al., 2025c). PRMs have further been adapted to sequential decision-making agents, where step rewards capture promise and progress rather than logical correctness (Xi et al., 2025). Finally, richer supervision signals beyond binary correctness have been explored: PathFinder-PRM introduces error-aware hierarchical supervision via explicit error typing (Pala et al., 2025; Jia et al., 2026). Data and evaluation issues have also been highlighted: the Qwen lessons show that Monte-Carlo-derived supervision can be noisy and that Best-of- $N$  evaluation can bias PRMs toward outcome-like behavior, motivating complementary step-level benchmarks (Zhang et al., 2025e), while PRMBench exposes fine-grained failure modes not captured by downstream reranking metrics alone (Song et al., 2025). Our work builds on this PRM literature but focuses on a specific, pervasive source of noise in multimodal settings: uncertainty in visual premises.

**Visual perception verification.** Modern MLLMs often fail to reliably *perceive* fine-grained visual facts (e.g., counting, geometry, structured reading) despite fluent outputs (Fu et al., 2024; Schulze Buschhoff et al., 2025).

This motivates stronger vision encoders (Jain et al., 2024), document-focused perception (Yu et al., 2024), and perception–language alignment training (Huang et al., 2023; Wu et al., 2024; Huang et al., 2025), as well as iterative perception schemes such as Chain-of-Visual-Perception (Tang et al., 2024) and Visual Perception Tokens (Yu et al., 2025). These efforts support our premise that verification should condition on the reliability of visual evidence.

**Multimodal process reward models.** Specialized multimodal PRMs have recently emerged as effective critics for test-time scaling. VisualPRM introduces large-scale multimodal process supervision and the VisualProcessBench benchmark, enabling systematic evaluation of step-level verification in vision-language reasoning (Wang et al., 2025b). Subsequent work improves data efficiency: ATHENA demonstrates that strong/weak consistency filtering and ORM initialization can produce competitive multimodal PRMs with substantially fewer labeled trajectories (Wang et al., 2025a), and broader analyses of VL-PRM training highlight practical lessons for scaling and deployment (Ong et al., 2025). Complementary efforts build multimodal PRM training pipelines and process supervision signals at scale (Luo et al., 2025; Cao et al., 2025). Beyond discriminative scoring, VRPRM combines chain-of-thought style verification with reinforcement learning to enhance multimodal process judgment (Chen et al., 2025), while GM-PRM extends verifiers with generative diagnosis and correction to support refined Best-of- $N$  (Zhang et al., 2025a). Tool-integrated verification provides another axis: TIM-PRM mitigates confirmation bias by independently querying visual evidence via tools, improving reliability but at a non-trivial inference cost (Kuang et al., 2025). Finally, broader evaluation efforts for vision-language reward modeling, including process- and critique-style settings, have been advanced by VLRMBench (Ruan et al., 2025). Across these approaches, multimodal PRMs are increasingly capable, yet the handling of *visual premise uncertainty* remains largely implicit: step scores are typically produced as if the underlying visual facts were equally reliable for all trajectories and all steps.

Prior work has advanced PRMs through stronger reasoning verifiers (She et al., 2025; Zhao et al., 2025; Khalifa et al., 2025; Guo et al., 2025), improved training objectives and data efficiency (Duan et al., 2025; Wang et al., 2025a; Zhang et al., 2025e, 2024b; Li & Li, 2024; Cheng et al., 2025), and tool-based evidence gathering for multimodal verification (Kuang et al., 2025). In contrast, our contribution targets a missing interface between perception and process supervision. We introduce *Explicit Visual Premise Verification* that (i) makes visual premises explicit via a policy-produced checklist, (ii) extracts structured visual constraints as independent evidence, and (iii) converts checklist–evidence consistency into a reliability signal used to calibrate step rewards. This decouples “whether the verifier can see” from “whether the step is logically correct,” reducing false positives/negatives under perceptual failures while remaining lightweight enough for large-scale Best-of- $N$  reranking.

## 3. Methodology

### 3.1. Problem Setup

Each instance consists of an image  $I$  and a question  $q$ . A multimodal policy produces a step-by-step solution  $S = (s_1, \dots, s_T)$  and final answer  $a$ . We aim to build a *process reward model* (PRM) that assigns a reward  $R_t \in [-1, 1]$  to each step  $s_t$ , supporting Best-of- $N$  reranking and step-level diagnosis.

The core difficulty in multimodal math is that errors come from two different sources: *visual grounding* (e.g., misread OCR/table values, wrong geometric relations, incorrect diagram structure) and *symbolic reasoning* (e.g., invalid derivations or arithmetic mistakes). Existing VL-PRMs typically output step scores directly, implicitly assuming the visual premise is reliable. When the premise is wrong early, later steps can remain locally coherent but globally invalid, and the verifier is forced to make confident judgments under uncertain perception. Our goal is to *separate* these error sources: we first assess whether the visual premise of a step is trustworthy, and only then rely on strict step correctness scores.

### 3.2. Explicit Visual Premise Verification (EVPV)

EVPV makes a PRM “qualified” to judge: it explicitly represents what visual facts a step relies on, checks those facts against independent visual evidence, and uses the resulting reliability to calibrate step rewards. Figure 2 summarizes the pipeline.

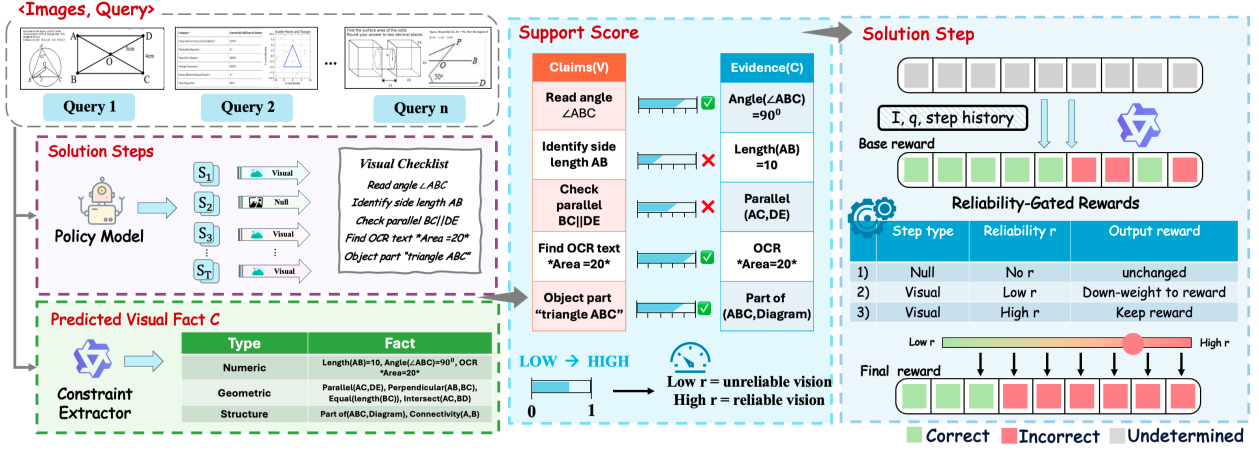


Figure 2 | **Overview of EVPV-PRM.** Given an image  $I$  and question  $q$ , the policy model generates a step-by-step solution and, for each step, declares whether it depends on visual evidence, forming a visual checklist of explicit claims. In parallel, a constraint extractor predicts a structured set of visual facts  $C$  (numeric readings, geometric relations, and compositional structure). We compute a visual reliability score  $r$  by matching checklist claims against  $C$  to obtain support scores and aggregating them into a single confidence signal. A step verifier then produces base step rewards, which are calibrated by reliability gating: rewards for non-visual steps are kept unchanged, while rewards for visually dependent steps are down-weighted when  $r$  is low and preserved when  $r$  is high. The resulting reliability-gated step rewards are aggregated for Best-of- $N$  reranking and process diagnosis.

### 3.2.1. Step-wise Visual Checklist

We ask the policy to accompany each step  $s_t$  with a short *visual premise* declaration:

$$d_t \in \{\text{a natural-language visual assertion, null}\}. \quad (1)$$

If  $d_t \neq \text{null}$ , the step claims dependence on a concrete visual fact (e.g., “the radius is 2”, “ $AB \perp CD$ ”, “the left part is attached by a cylinder”). We mark visual dependency by

$$v_t = \mathbb{1}[d_t \neq \text{null}] \in \{0, 1\}. \quad (2)$$

Collecting all non-null declarations yields a *visual checklist*  $V = \{v_j\}_{j=1}^M$ . This checklist is the interface EVPV needs: it turns implicit visual assumptions into explicit claims that can be verified independently from the policy’s later algebra.

### 3.2.2. Structured Visual Evidence (Constraints)

To verify the checklist, we extract structured visual evidence from the image once per instance using a constraint extractor  $E_\phi$ :

$$C = E_\phi(I, q) = \{c_k\}_{k=1}^K. \quad (3)$$

Each constraint follows a unified JSON schema (Appendix A) that covers (i) numeric readings (lengths, angles, table entries), (ii) relations (parallel/perpendicular/equality/incidence/containment), and (iii) compositional structure (part-whole, attachments, adjacency). Importantly, at test time EVPV relies only on the predicted  $C$ ; no gold facts are used.

### 3.2.3. Consistency-to-Reliability

EVPV converts checklist–evidence consistency into a scalar *visual reliability* score. Let  $m(\cdot)$  be a type-aware matching function that measures whether a checklist claim is supported by  $C$ :

$$p_j = m(v_j, C) \in [0, 1], \quad (4)$$

where  $p_j$  is high when the claim is entailed by extracted constraints (with numeric tolerance and entity/relation alignment; Appendix B).

We then aggregate  $\{p_j\}$  into a single reliability value

$$r = \text{Agg}(p_1, \dots, p_M) \in [0, 1]. \quad (5)$$

Because a single catastrophic misread can invalidate the entire trace, Agg should be sensitive to strongly unsupported claims. We use a robust geometric aggregation:

$$r = \exp\left(\frac{1}{M} \sum_{j=1}^M \log(\epsilon + p_j)\right), \quad (6)$$

with a small  $\epsilon$  for stability. Under hallucinated structure or misread values, one or more  $p_j$  drops sharply, pulling  $r$  down; when the checklist is well supported,  $r$  remains high.

### 3.3. Step Verification with Reliability-Gated Rewards

**Base step verifier.** We train a standard step verifier  $V_\theta$  to predict whether step  $s_t$  is correct given the multimodal context and prefix:

$$u_t = P_\theta(y_t = 1 \mid I, q, s_{\leq t}) \in [0, 1], \quad (7)$$

where  $y_t = 1$  indicates a correct step. We map this probability to a signed base reward:

$$R_t^{\text{base}} = 2u_t - 1 \in [-1, 1]. \quad (8)$$

**Reliability gating (EVPV calibration).** A base verifier score alone is ambiguous in multimodal settings: a low score may reflect a true logical error, or simply that the step rests on a misperceived visual premise (either by the policy or by the verifier). EVPV resolves this ambiguity by *calibrating* rewards for visually dependent steps using  $r$ .

We convert reliability into a smooth gating factor

$$\alpha(r) = \sigma(\beta(r - \tau)) \in (0, 1), \quad (9)$$

where  $\tau$  is a reliability threshold,  $\beta$  controls smoothness, and  $\sigma$  is the logistic function. The final step reward is

$$R_t = \begin{cases} R_t^{\text{base}}, & \nu_t = 0, \\ \alpha(r) R_t^{\text{base}}, & \nu_t = 1. \end{cases} \quad (10)$$

This implements a simple principle: *when the visual premise is unreliable, do not over-interpret step correctness*. If  $r \ll \tau$ , then  $\alpha(r) \approx 0$  and visually grounded steps are pushed toward neutral reward, preventing early perceptual failures from producing overly confident negative (or positive) signals that destabilize reranking and diagnosis. If  $r \gg \tau$ , then  $\alpha(r) \approx 1$  and the verifier behaves like a conventional PRM.

**Trajectory scoring for Best-of- $N$ .** Given a candidate solution  $S$ , we compute  $\{R_t\}_{t=1}^T$  and aggregate into a trajectory score. Unless stated otherwise, we use the fraction of positively rewarded steps:

$$\text{Score}(S) = \frac{1}{T} \sum_{t=1}^T \mathbb{1}[R_t > 0], \quad (11)$$

and select the candidate with the highest score. We report alternative aggregations in Appendix E.

### 3.4. Training

EVPV introduces two trainable modules: the constraint extractor  $E_\phi$  and the step verifier  $V_\theta$ . The policy is not trained in this work; it is only prompted to output steps and checklist items at inference (Figure 3).

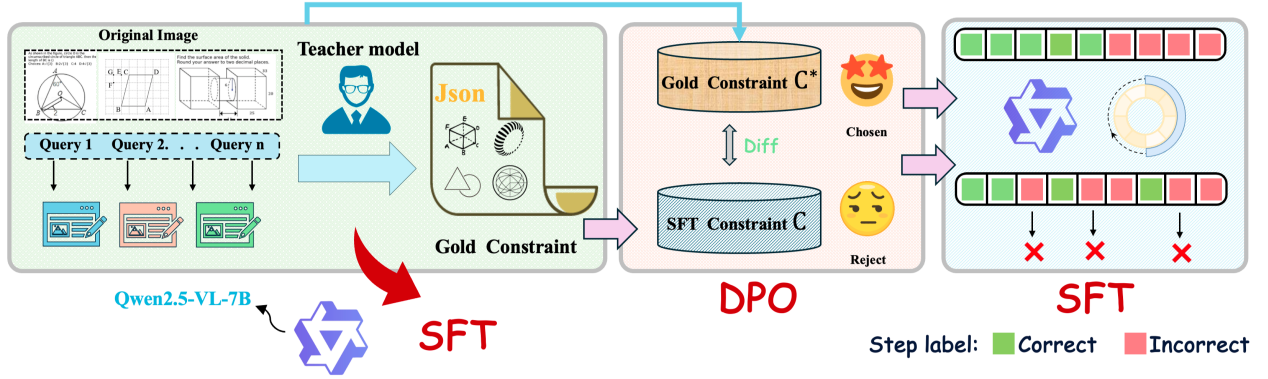


Figure 3 | **Training pipeline for the constraint extractor and step verifier.** We train the constraint extractor  $E_\phi$  by distilling gold structured constraints  $C^*$  from a strong teacher on image–question inputs (here, 20K samples from VisualPRM400K with `qwen3-vl-235b-a22b-instruct`), using supervised fine-tuning with  $\mathcal{L}_{\text{con}} = -\log P_\phi(C^* | I, q)$ . After SFT initialization, we construct preference pairs by letting  $E_\phi$  generate candidate constraints and selecting hard cases where the teacher identifies large deviations from  $C^*$ ; we then apply DPO to improve constraint fidelity. In parallel, we train the step verifier  $V_\theta$  with step-level correctness labels via binary cross-entropy. Gold constraints are used only during training; inference relies solely on predicted constraints and checklist consistency.

**Training the constraint extractor.** We distill structured constraints from a strong teacher model. For each training instance, the teacher provides a constraint set  $C^*$  (we use `qwen3-vl-235b-a22b-instruct` on 20K samples from VisualPRM400K). We fine-tune  $E_\phi$  with:

$$\mathcal{L}_{\text{con}}(\phi) = -\log P_\phi(C^* | I, q), \quad (12)$$

where  $C^*$  is serialized as JSON.

To improve fidelity on hard cases, we further apply DPO. We sample candidates  $\{C^{(i)}\}_{i=1}^n \sim P_\phi(\cdot | I, q)$  and form a preferred/rejected pair  $(C^+, C^-)$  using a schema-aware distance to  $C^*$  (Appendix A,B). The DPO loss is:

$$\mathcal{L}_{\text{DPO}}(\phi) = -\log \sigma\left(\beta_{\text{dpo}} \left[ \log P_\phi(C^+ | I, q) - \log P_\phi(C^- | I, q) \right]\right), \quad (13)$$

and the full extractor objective is

$$\mathcal{L}_E(\phi) = \mathcal{L}_{\text{con}}(\phi) + \lambda_{\text{dpo}} \mathcal{L}_{\text{DPO}}(\phi). \quad (14)$$

**Training the step verifier.** We train  $V_\theta$  with step-level correctness labels using binary cross-entropy:

$$\mathcal{L}_V(\theta) = -\sum_{t=1}^T \left( y_t \log u_t + (1 - y_t) \log(1 - u_t) \right), \quad (15)$$

where  $u_t = P_\theta(y_t = 1 | I, q, s_{\leq t})$ . Reliability  $r$  and gating (Equation (10)) are applied at inference time as a calibration layer, keeping verifier training simple and making EVPV easy to plug into existing PRMs.

**Inference.** For each candidate solution, we (i) obtain steps and checklist from the policy, (ii) predict constraints  $C = E_\phi(I, q)$  once, (iii) compute reliability  $r$  by matching checklist items to  $C$ , (iv) compute gated step rewards via Equations (8) and (10), and (v) aggregate rewards to rerank candidates. This achieves premise-aware verification without step-wise tool calls.

## 4. Experiments

### 4.1. Benchmarks, Protocol, and Baselines

We evaluate EVPV from two angles: (i) *step-level verification* on annotated reasoning traces, and (ii) *deployable test-time gains* under Best-of- $N$  reranking. For step-level evaluation we use **VisualProcessBench** (Wang et al.,

Table 1 | VisualProcessBench Macro-F1 (%). *Yes*: judge receives our structured constraints; *No*: original prompt;  $\Delta = \text{Yes} - \text{No}$  (in points). Positive  $\Delta$  is highlighted.

Model		DynaMath	MMMU	MathVerse	MathVision	WeMath	Overall
<b>Proprietary Models</b>							
gpt-4o-mini	No	56.57	54.08	52.53	51.42	56.74	53.57
	Yes	58.13	53.20	54.09	52.07	54.62	54.29
	$\Delta$	<b>+1.56</b>	-0.88	<b>+1.56</b>	<b>+0.65</b>	-2.12	<b>+0.72</b>
doubao-seed-1.6-vision	No	66.19	59.47	63.12	61.07	62.74	62.77
	Yes	68.66	61.86	65.57	62.51	64.62	64.91
	$\Delta$	<b>+2.47</b>	<b>+2.39</b>	<b>+2.45</b>	<b>+1.44</b>	<b>+1.88</b>	<b>+2.14</b>
Gemini 2.5 Pro	No	68.47	63.34	68.26	65.15	69.48	67.13
	Yes	71.32	64.42	69.78	65.26	72.43	68.64
	$\Delta$	<b>+2.85</b>	<b>+1.08</b>	<b>+1.52</b>	<b>+0.11</b>	<b>+2.95</b>	<b>+1.51</b>
<b>Open-source Models</b>							
qwen2.5-vl-72b-instruct	No	56.99	59.43	56.43	58.09	55.72	57.19
	Yes	61.43	60.25	59.85	59.12	59.72	59.99
	$\Delta$	<b>+4.44</b>	<b>+0.82</b>	<b>+3.42</b>	<b>+1.03</b>	<b>+4.00</b>	<b>+2.80</b>
Qwen3-VL-30B-A3B-instruct	No	58.95	61.29	57.37	57.49	58.76	58.22
	Yes	62.27	59.00	59.68	56.49	59.50	59.26
	$\Delta$	<b>+3.32</b>	-2.29	<b>+2.31</b>	-1.00	<b>+0.74</b>	<b>+1.04</b>
Qwen3-VL-235B-A22B-instruct	No	57.63	58.73	58.08	59.59	58.76	58.51
	Yes	68.43	61.54	65.97	64.54	64.16	65.45
	$\Delta$	<b>+10.80</b>	<b>+2.81</b>	<b>+7.89</b>	<b>+4.95</b>	<b>+5.40</b>	<b>+6.94</b>
<b>Process Reward Models</b>							
QWEN-VL-PRM-7B (Ong et al., 2025)		58.30	55.80	58.80	55.70	59.80	58.60
TIM-PRM-8B (Kuang et al., 2025)		65.90	58.30	61.90	58.30	63.90	61.70
VisualPRM-8B (Wang et al., 2025b)		62.70	58.50	61.00	62.10	61.80	62.00
EVPV-PRM		<b>69.57</b>	<b>68.86</b>	<b>67.09</b>	<b>65.27</b>	<b>69.11</b>	<b>67.46</b>

2025b). For downstream evaluation we use six multimodal reasoning benchmarks: LogicVista (Xiao et al., 2024), MMMU (Yue et al., 2024), MathVerse-VO (Zhang et al., 2024c), MathVision (Wang et al., 2024), MathVista (Lu et al., 2023), and WeMath (Qiao et al., 2025).

**Metrics.** On VisualProcessBench we report step-level **Macro-F1** (primary) and accuracy. On downstream benchmarks we report **Pass@1** (policy accuracy without reranking), **BoN@k** (accuracy after reranking  $k$  samples), and the practical gain  $\Delta_k = \text{BoN@k} - \text{Pass@1}$ . We also report **Std Pass@k**, the oracle upper bound of the candidate set, to separate candidate quality from selection quality.

**Baselines.** We compare against multimodal PRMs including **VisualPRM** (Wang et al., 2025b), **QWEN-VL-PRM-7B** (Ong et al., 2025) and the tool-integrated verifier **TIM-PRM** (Kuang et al., 2025). We also evaluate several strong MLLMs as step judges under a standardized prompt, with two conditions: *No* (original prompt) and *Yes* (append our extracted structured constraints as evidence). Finally, we include component ablations of EVPV (checklist, constraints, matching, gating).

#### 4.2. Exp-1: Step Verification on VisualProcessBench

We evaluate step-level verification directly on VisualProcessBench (Wang et al., 2025b). Table 1 compares our method with prior multimodal PRMs and a set of judge models. For judge models, *Yes* appends our extracted structured constraints, while *No* uses the original prompt.

Two observations stand out in Table 1. First, our method achieves the best overall Macro-F1 among the compared PRMs, indicating stronger step discrimination under real visual uncertainty. Second, many judge models improve under *Yes*, suggesting that the constraint representation is broadly reusable as external evidence—even without retraining the judge—and that a non-trivial part of verification error comes from missing or unreliable grounding.

Table 2 | **Downstream Best-of-8 reranking with InternVL2.5 policies.** BoN@8 accuracy (%) after reranking with different PRMs; red numbers denote  $\Delta_8$  (BoN@8 – Pass@1) for our PRM.

Model	MathVista	MathVision	MathVerse-VO	WeMath	LogicVista	MMMU	Overall
<b>Proprietary Models</b>							
GPT-4o	60.00	31.20	40.60	45.80	52.80	70.70	47.90
Gemini-2.0-Flash	70.40	43.60	47.80	47.40	52.30	69.90	53.40
Claude-3.5-Sonnet	65.30	35.60	46.30	44.00	60.40	66.40	50.50
<b>Open-source Models</b>							
InternVL2.5-8B	64.50	17.00	22.80	23.50	36.38	56.20	32.84
+VisualPRM	68.50	25.70	35.80	36.50	43.80	60.20	41.40
	+4.00	+8.70	+13.00	+13.00	+7.80	+4.00	+8.40
+EVPV-PRM	76.30	22.07	29.47	37.45	45.33	67.75	41.67
	<b>+11.80</b>	<b>+5.07</b>	<b>+6.67</b>	<b>+13.95</b>	<b>+8.95</b>	<b>+11.55</b>	<b>+8.83</b>
InternVL2.5-26B	68.20	23.40	24.00	30.90	39.64	60.70	37.23
+VisualPRM	73.10	29.60	39.10	40.80	51.00	63.90	45.80
	+4.90	+6.20	+15.10	+9.90	+11.40	+3.20	+8.90
+EVPV-PRM	79.60	28.11	32.47	42.14	51.72	69.25	46.75
	<b>+11.40</b>	<b>+4.71</b>	<b>+8.47</b>	<b>+11.24</b>	<b>+12.08</b>	<b>+8.55</b>	<b>+9.52</b>
InternVL2.5-38B	71.90	32.20	36.90	38.30	47.90	63.90	45.44
+VisualPRM	73.90	35.20	46.70	46.20	53.70	69.00	50.70
	+2.00	+3.00	+9.80	+7.90	+5.80	+5.10	+6.30
+EVPV-PRM	83.50	37.59	47.67	50.00	58.74	72.33	55.22
	<b>+11.60</b>	<b>+5.39</b>	<b>+10.77</b>	<b>+11.70</b>	<b>+10.84</b>	<b>+8.43</b>	<b>+9.78</b>

### 4.3. Exp-2: Best-of- $N$ Reranking in Downstream Benchmarks

We next test whether premise-aware verification translates into deployable test-time gains. We rerank candidates generated by InternVL2.5 policy models at three scales (8B/26B/38B). For each question, the policy samples  $k \in \{1, \dots, 8\}$  candidate solutions; we rerank them using step rewards and report BoN@8.

Table 2 summarizes the results. Across all three policy sizes, our PRM yields consistent gains over the base policy and improves upon VisualPRM (Wang et al., 2025b) in overall performance (e.g., +8.83, +9.52, and +9.78 points over Pass@1 for 8B/26B/38B, respectively). The improvements are especially pronounced on visually intensive benchmarks such as MathVista, WeMath, and LogicVista, which matches EVPV’s intent: when early visual premises are the dominant failure mode, reliability-aware step scoring reduces selection errors without incurring the per-step tool overhead of TIM-PRM (Kuang et al., 2025).

### 4.4. Exp-3: Perception Evidence Quality and Its Causal Impact on Verification

EVPV is motivated by a single principle: *reliable visual evidence is a prerequisite for meaningful process verification*. We therefore examine this principle from two complementary angles—(i) **intervention on the policy’s perceived evidence** and (ii) **controlled degradation of the verifier’s extracted constraints**—to quantify both the sensitivity of multimodal reasoning to perception and the causal role of constraint fidelity in step verification.

**(A) Perception interventions for the policy.** To measure how strongly multimodal reasoning depends on perception quality, we evaluate the *same* questions under four controlled settings: (I) **Normal** (image+ $q$ ), (II) **Oracle perception** (image+ $q$  plus an oracle structured description), (III) **Noisy perception** (image+ $q$  plus a corrupted description), and (IV) **Text-only** (remove the image). We run a fixed policy model for all settings and report answer accuracy and PRM trajectory scores. Table 3 shows two consistent patterns: providing **oracle perception** substantially improves accuracy, while **text-only** performance drops sharply, indicating that perception is a dominant bottleneck; moreover, our PRM yields a **monotonic ordering of trajectory scores**

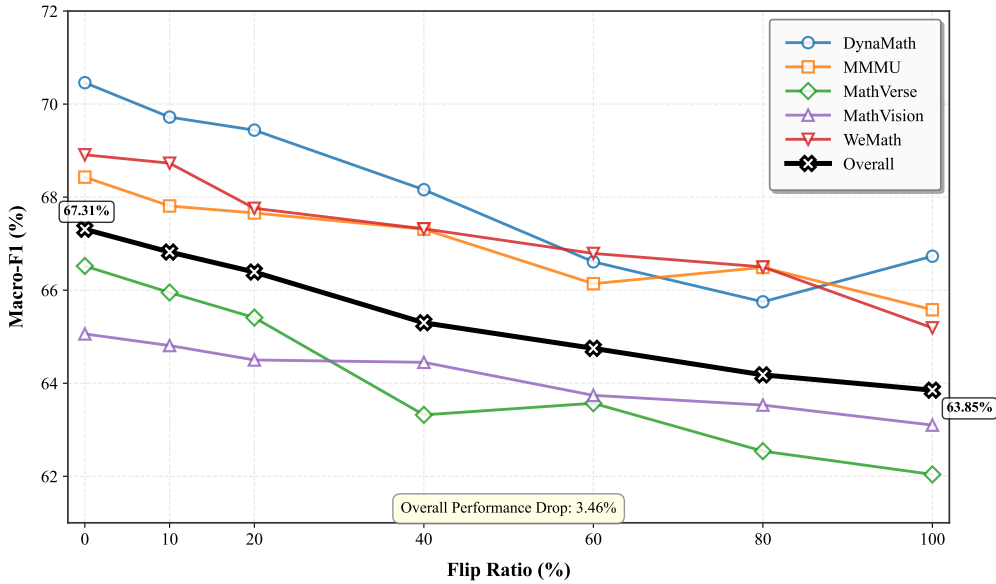


Figure 4 | Constraint quality–performance causal curves under controlled noise.

Table 3 | Perception interventions. We evaluate the same questions under four perception conditions by InternVL2.5-8B. **Top:** policy accuracy (%). **Bottom:** average PRM trajectory score (higher is better).

Condition		LogicVista	MathVerse-VO	MathVision
<b>Acc. (%)</b>				
(I)	Normal	38.26	24.54	15.86
(II)	Oracle perception	48.10	38.48	23.75
(III)	Noisy perception	40.49	32.46	18.82
(IV)	Text-only	21.25	16.22	12.50
<b>Score</b>				
(I)	Normal	0.08	0.22	0.05
(II)	Oracle perception	0.20	0.45	0.19
(III)	Noisy perception	0.10	0.34	0.09
(IV)	Text-only	-0.31	-0.11	-0.01

aligned with perception quality: (II)>(III)>(I)>(IV), matching EVPV’s intent that weakened visual evidence should not produce a strong “correct process” signal.

**(B) Causal curve via constraint corruption.** EVPV further attributes its gains to the fidelity of the extracted structured constraints used to validate checklist claims. To test this causally, we inject controlled noise into the constraint set by randomly flipping a fraction of constraint fields (flip ratio), while keeping the policy, verifier architecture, and scoring procedure fixed. As shown in Figure 4, VisualProcessBench Macro-F1 decreases monotonically as the flip ratio increases across all evaluated judges, providing causal evidence that verification quality is driven by **constraint fidelity and premise verification** rather than incidental prompt length or formatting effects. The mild drop under low noise also indicates that the reliability gating is not overly brittle: small constraint errors do not immediately collapse step judgments.

#### 4.5. Exp-4: Ablation Studies

We ablate core components of EVPV to identify which parts are responsible for the verification and reranking gains. Table 4 reports representative variants on VisualProcessBench (Macro-F1).

The trends closely match the EVPV design. First, premise verification requires *usable structured evidence*. Replacing structured constraints with caption-only descriptions reduces overall Macro-F1 by 4.08 points, and

Table 4 | Key ablations on VisualProcessBench (Macro-F1; higher is better).  $\Delta$  is relative to the full method.

Variant	DynaMath	MMMU	MathVerse	MathVision	WeMath	Overall	$\Delta$
<b>Full Method</b>							
Full (EVPV + gating)	69.57	68.86	67.09	65.27	69.11	67.46	+0.00
<b>Evidence / structure ablations</b>							
w/o structured facts (caption-only)	67.75	58.09	63.48	60.68	67.10	63.38	-4.08
w/o constraints (facts = $\emptyset$ )	66.66	55.80	62.61	59.13	65.81	62.11	-5.35
w/ shuffled facts (structure corrupted)	62.86	52.57	59.81	58.52	64.77	59.82	-7.64
<b>Remove modalities / severe corruption</b>							
w/o vision (text-only judge, keep JSON)	58.44	49.44	53.59	54.07	61.02	54.93	-12.53
w/o vision & w/o JSON (text-only)	54.49	43.93	42.78	50.84	53.78	48.23	-19.23
w/ drop-facts corruption	34.90	34.40	36.29	36.14	35.96	35.77	-31.69

completely removing constraints (facts =  $\emptyset$ ) further degrades performance (-5.35). This shows that simply having additional text context is insufficient; the verifier benefits from structured, matchable facts that can support checklist claims.

*structure and alignment matter.* When we keep the same facts but shuffle them to corrupt the relational structure, Macro-F1 drops more sharply (-7.64). This indicates that EVPV is not merely exploiting the presence of extra tokens, but relies on faithful entity/relation alignment between checklist items and evidence to compute reliability and gate rewards appropriately.

EVPV still depends on *direct visual access*. Making the judge text-only while keeping the JSON constraints causes a large drop (-12.53), and removing both vision and JSON drops further (-19.23). Thus, structured constraints are helpful but do not fully substitute for image-conditioned verification; both modalities contribute to reliable step supervision. Finally, the drop-facts corruption collapses performance (-31.69), reflecting that when evidence becomes severely incomplete, the verifier is effectively ungrounded and reliability gating can no longer provide meaningful calibration.

## 5. Discussion

**Why EVPV helps: turning a hidden assumption into a checked premise.** Most process reward models score a step as if the underlying facts were settled, even though in multimodal problems the “facts” often come from fragile perception. This creates a systematic ambiguity: a low score may reflect wrong logic, or simply a misread diagram. EVPV reduces this ambiguity by making visual premises explicit (checklist) and verifying them against independent structured evidence (constraints) before trusting strict step judgments. This view aligns with findings that multimodal chain-of-thought reliability depends on faithful visual grounding (Zhang et al., 2025b) and with “generate-then-verify” interventions that explicitly validate claims to mitigate hallucinations (Wu et al., 2025). The controlled perception intervention in Table 3 supports this premise: as perception quality changes, answer accuracy and our trajectory scores shift coherently.

**From verification to deployment: more reliable reranking under test-time scaling.** The reranking results in Table 2 show that premise-aware scoring yields practical gains across InternVL2.5 policy sizes, with the largest improvements on benchmarks where early visual misreads dominate. This suggests EVPV mainly reduces *selection errors*—fluent but visually wrong traces being ranked above grounded ones. Compared with tool-integrated verification (e.g., TIM-PRM (Kuang et al., 2025)), EVPV is lightweight: it validates premises once per problem via extracted constraints, avoiding expensive per-step tool calls, while remaining compatible with verification-driven test-time reliability strategies (Wu et al., 2025).

**Evidence quality matters, and the ablations isolate it.** Our gains are driven by premise verification with usable structured evidence. Step-level improvements on VisualProcessBench (Table 1) and the monotonic degradation under constraint corruption (Figure 4) indicate a direct dependence on constraint fidelity, and the ablations (Table 4) show that removing structured facts or vision substantially harms performance. These results complement analyses that PRM robustness depends on controlling supervision noise (Zheng et al., 2025);

Wang et al., 2025a) and are consistent with recent efforts to stabilize process-level signals via redesigned step-wise learning objectives (Fei et al., 2025).

## 6. Conclusion

We introduced Explicit Visual Premise Verification (EVPV) for multimodal process reward modeling. EVPV prompts the policy to state step-wise visual premises, verifies them against structured constraints extracted from the image, and uses the resulting reliability signal to calibrate step rewards. This decoupling makes process supervision more dependable under perceptual failures and improves Best-of- $N$  selection in downstream multimodal reasoning.

EVPV has limitations. Its effectiveness depends on the coverage and accuracy of the extracted constraints: missing or spurious constraints can under- or over-gate visually grounded steps. It also relies on checklist quality; incomplete or overly vague premises reduce matchability, and instance-level reliability may be coarse for traces that mix local visual reads with pure algebra. Future work includes step-/claim-conditioned reliability (rather than a single global signal), uncertainty-aware constraint extraction and matching, and integrating premise-aware rewards into training-time process optimization to further improve robustness under distribution shift and long-horizon reasoning.

## References

- Qi Cao, Ruiyi Wang, Ruiyi Zhang, Sai Ashish Somayajula, and Pengtao Xie. Dreamprm: Domain-reweighted process reward model for multimodal reasoning. *arXiv preprint arXiv:2505.20241*, 2025.
- Xinquan Chen, Bangwei Liu, Xuhong Wang, Yingchun Wang, and Chaochao Lu. Vrprm: Process reward modeling via visual reasoning. *arXiv preprint arXiv:2508.03556*, 2025.
- Jie Cheng, Gang Xiong, Ruixi Qiao, Lijun Li, Chao Guo, Junle Wang, Yisheng Lv, and Fei-Yue Wang. Stop summation: Min-form credit assignment is all process reward model needs for reasoning. *arXiv preprint arXiv:2504.15275*, 2025.
- Keyu Duan, Zichen Liu, Xin Mao, Tianyu Pang, Changyu Chen, Qiguang Chen, Michael Qizhe Shieh, and Longxu Dou. Efficient process reward model training via active learning. *arXiv preprint arXiv:2504.10559*, 2025.
- Wu Fei, Hao Kong, Shuxian Liang, Yang Lin, Yibo Yang, Jing Tang, Lei Chen, and Xiansheng Hua. Self-guided process reward optimization with redefined step-wise advantage for process reinforcement learning. *arXiv preprint arXiv:2507.01551*, 2025.
- Xingyu Fu, Yushi Hu, Bangzheng Li, Yu Feng, Haoyu Wang, Xudong Lin, Dan Roth, Noah A Smith, Wei-Chiu Ma, and Ranjay Krishna. Blink: Multimodal large language models can see but not perceive. In *European Conference on Computer Vision*, pp. 148–166. Springer, 2024.
- Jiaxin Guo, Zewen Chi, Li Dong, Qingxiu Dong, Xun Wu, Shaohan Huang, and Furu Wei. Reward reasoning model. *arXiv preprint arXiv:2505.14674*, 2025.
- Jiaxing Huang, Jingyi Zhang, Kai Jiang, Han Qiu, Xiaoqin Zhang, Ling Shao, Shijian Lu, and Dacheng Tao. Visual instruction tuning towards general-purpose multimodal large language model: A survey. *International Journal of Computer Vision*, 133(11):8151–8189, 2025.
- Shaohan Huang, Li Dong, Wenhui Wang, Yaru Hao, Saksham Singhal, Shuming Ma, Tengchao Lv, Lei Cui, Owais Khan Mohammed, Barun Patra, et al. Language is not all you need: Aligning perception with language models. *Advances in Neural Information Processing Systems*, 36:72096–72109, 2023.
- Jitesh Jain, Jianwei Yang, and Humphrey Shi. Vcoder: Versatile vision encoders for multimodal large language models. In *Proceedings of the IEEE/CVF Conference on Computer Vision and Pattern Recognition*, pp. 27992–28002, 2024.

- Ruipeng Jia, Yunyi Yang, Yongbo Gai, Kai Luo, Shihao Huang, Jianhe Lin, Xiaoxi Jiang, and Guanjun Jiang. Writing-zero: Bridge the gap between non-verifiable tasks and verifiable rewards. *arXiv preprint arXiv:2506.00103*, 2025.
- Ruipeng Jia, Yunyi Yang, Yuxin Wu, Yongbo Gai, Siyuan Tao, Mengyu Zhou, Jianhe Lin, Xiaoxi Jiang, and Guanjun Jiang. Open rubric system: Scaling reinforcement learning with pairwise adaptive rubric. *arXiv preprint arXiv:2602.14069*, 2026.
- Muhammad Khalifa, Rishabh Agarwal, Lajanugen Logeswaran, Jaekyeom Kim, Hao Peng, Moontae Lee, Honglak Lee, and Lu Wang. Process reward models that think. *arXiv preprint arXiv:2504.16828*, 2025.
- Peng Kuang, Xiangxiang Wang, Wentao Liu, Jian Dong, and Kaidi Xu. Tim-prm: Verifying multimodal reasoning with tool-integrated prm. *arXiv preprint arXiv:2511.22998*, 2025.
- Wendi Li and Yixuan Li. Process reward model with q-value rankings. *arXiv preprint arXiv:2410.11287*, 2024.
- Pan Lu, Hritik Bansal, Tony Xia, Jiacheng Liu, Chunyuan Li, Hannaneh Hajishirzi, Hao Cheng, Kai-Wei Chang, Michel Galley, and Jianfeng Gao. Mathvista: Evaluating mathematical reasoning of foundation models in visual contexts. *arXiv preprint arXiv:2310.02255*, 2023.
- Ruilin Luo, Zhuofan Zheng, Yifan Wang, Xinzhe Ni, Zicheng Lin, Songtao Jiang, Yiyao Yu, Chufan Shi, Lei Wang, Ruihang Chu, et al. Unlocking multimodal mathematical reasoning via process reward model. *arXiv preprint arXiv:2501.04686*, 2025.
- Qianli Ma, Haotian Zhou, Tingkai Liu, Jianbo Yuan, Pengfei Liu, Yang You, and Hongxia Yang. Let’s reward step by step: Step-level reward model as the navigators for reasoning. *arXiv preprint arXiv:2310.10080*, 2023.
- Brandon Ong, Tej Deep Pala, Vernon Toh, William Chandra Tjhi, and Soujanya Poria. Training vision-language process reward models for test-time scaling in multimodal reasoning: Key insights and lessons learned. *arXiv preprint arXiv:2509.23250*, 2025.
- Tej Deep Pala, Panshul Sharma, Amir Zadeh, Chuan Li, and Soujanya Poria. Error typing for smarter rewards: Improving process reward models with error-aware hierarchical supervision. *arXiv preprint arXiv:2505.19706*, 2025.
- Young-Jin Park, Kristjan Greenewald, Kaveh Alim, Hao Wang, and Navid Azizan. Know what you don’t know: Uncertainty calibration of process reward models. *arXiv preprint arXiv:2506.09338*, 2025.
- Runqi Qiao, Qiuna Tan, Guanting Dong, MinhuiWu MinhuiWu, Chong Sun, Xiaoshuai Song, Jiapeng Wang, Zhuoma Gongque, Shanglin Lei, Yifan Zhang, et al. We-math: Does your large multimodal model achieve human-like mathematical reasoning? In *Proceedings of the 63rd Annual Meeting of the Association for Computational Linguistics (Volume 1: Long Papers)*, pp. 20023–20070, 2025.
- Jiacheng Ruan, Wenzhen Yuan, Xian Gao, Ye Guo, Daoxin Zhang, Zhe Xu, Yao Hu, Ting Liu, and Yuzhuo Fu. Vlrm-bench: A comprehensive and challenging benchmark for vision-language reward models. In *Proceedings of the IEEE/CVF International Conference on Computer Vision*, pp. 3163–3173, 2025.
- Luca M Schulze Buschoff, Elif Akata, Matthias Bethge, and Eric Schulz. Visual cognition in multimodal large language models. *Nature Machine Intelligence*, 7(1):96–106, 2025.
- Shuaijie She, Junxiao Liu, Yifeng Liu, Jiajun Chen, Xin Huang, and Shujian Huang. R-prm: Reasoning-driven process reward modeling. *arXiv preprint arXiv:2503.21295*, 2025.
- Mingyang Song, Zhaochen Su, Xiaoye Qu, Jiawei Zhou, and Yu Cheng. Prmbench: A fine-grained and challenging benchmark for process-level reward models. *arXiv preprint arXiv:2501.03124*, 2025.
- Xiaoyu Tan, Tianchu Yao, Chao Qu, Bin Li, Minghao Yang, Dakuan Lu, Haozhe Wang, Xihe Qiu, Wei Chu, Yinghui Xu, et al. Aurora: Automated training framework of universal process reward models via ensemble prompting and reverse verification. *arXiv preprint arXiv:2502.11520*, 2025.

- Lv Tang, Peng-Tao Jiang, Zhi-Hao Shen, Hao Zhang, Jin-Wei Chen, and Bo Li. Chain of visual perception: Harnessing multimodal large language models for zero-shot camouflaged object detection. In *Proceedings of the 32nd ACM international conference on multimedia*, pp. 8805–8814, 2024.
- Ke Wang, Junting Pan, Weikang Shi, Zimu Lu, Houxing Ren, Aojun Zhou, Mingjie Zhan, and Hongsheng Li. Measuring multimodal mathematical reasoning with math-vision dataset. *Advances in Neural Information Processing Systems*, 37:95095–95169, 2024.
- Shuai Wang, Zhenhua Liu, Jiaheng Wei, Xuanwu Yin, Dong Li, and Emad Barsoum. Athena: Enhancing multimodal reasoning with data-efficient process reward models. *arXiv preprint arXiv:2506.09532*, 2025a.
- Weiyun Wang, Zhangwei Gao, Lianjie Chen, Zhe Chen, Jinguo Zhu, Xiangyu Zhao, Yangzhou Liu, Yue Cao, Shenglong Ye, Xizhou Zhu, et al. Visualprm: An effective process reward model for multimodal reasoning. *arXiv preprint arXiv:2503.10291*, 2025b.
- Giannan Wu, Muyan Zhong, Sen Xing, Zeqiang Lai, Zhaoyang Liu, Zhe Chen, Wenhai Wang, Xizhou Zhu, Lewei Lu, Tong Lu, et al. Visionllm v2: An end-to-end generalist multimodal large language model for hundreds of vision-language tasks. *Advances in Neural Information Processing Systems*, 37:69925–69975, 2024.
- Tsung-Han Wu, Heekyung Lee, Jiabin Ge, Joseph E Gonzalez, Trevor Darrell, and David M Chan. Generate, but verify: Reducing hallucination in vision-language models with retrospective resampling. *arXiv preprint arXiv:2504.13169*, 2025.
- Zhiheng Xi, Chenyang Liao, Guanyu Li, Yajie Yang, Wenxiang Chen, Zhihao Zhang, Binghai Wang, Senjie Jin, Yuhao Zhou, Jian Guan, et al. Agentprm: Process reward models for llm agents via step-wise promise and progress. *arXiv preprint arXiv:2511.08325*, 2025.
- Yijia Xiao, Edward Sun, Tianyu Liu, and Wei Wang. Logicvista: Multimodal llm logical reasoning benchmark in visual contexts. *arXiv preprint arXiv:2407.04973*, 2024.
- Zihuiwen Ye, Luckeciano Carvalho Melo, Younesse Kaddar, Phil Blunsom, Sam Staton, and Yarin Gal. Uncertainty-aware step-wise verification with generative reward models. *arXiv preprint arXiv:2502.11250*, 2025.
- Zhangyue Yin, Qiushi Sun, Zhiyuan Zeng, Qinyuan Cheng, Xipeng Qiu, and Xuan-Jing Huang. Dynamic and generalizable process reward modeling. In *Proceedings of the 63rd Annual Meeting of the Association for Computational Linguistics (Volume 1: Long Papers)*, pp. 4203–4233, 2025.
- Runpeng Yu, Xinyin Ma, and Xinchao Wang. Introducing visual perception token into multimodal large language model. *arXiv preprint arXiv:2502.17425*, 2025.
- Ya-Qi Yu, Minghui Liao, Jihao Wu, Yongxin Liao, Xiaoyu Zheng, and Wei Zeng. Texthawk: Exploring efficient fine-grained perception of multimodal large language models. *arXiv preprint arXiv:2404.09204*, 2024.
- Xiang Yue, Yuansheng Ni, Kai Zhang, Tianyu Zheng, Ruoqi Liu, Ge Zhang, Samuel Stevens, Dongfu Jiang, Weiming Ren, Yuxuan Sun, et al. Mmmu: A massive multi-discipline multimodal understanding and reasoning benchmark for expert agi. In *Proceedings of the IEEE/CVF Conference on Computer Vision and Pattern Recognition*, pp. 9556–9567, 2024.
- Thomas Zeng, Shuibai Zhang, Shutong Wu, Christian Classen, Daewon Chae, Ethan Ewer, Minjae Lee, Heeju Kim, Wonjun Kang, Jackson Kunde, et al. Versaprm: Multi-domain process reward model via synthetic reasoning data. *arXiv preprint arXiv:2502.06737*, 2025.
- Dan Zhang, Sining Zhoubian, Ziniu Hu, Yisong Yue, Yuxiao Dong, and Jie Tang. Rest-mcts\*: Llm self-training via process reward guided tree search. *Advances in Neural Information Processing Systems*, 37:64735–64772, 2024a.
- Hanning Zhang, Pengcheng Wang, Shizhe Diao, Yong Lin, Rui Pan, Hanze Dong, Dylan Zhang, Pavlo Molchanov, and Tong Zhang. Entropy-regularized process reward model. *arXiv preprint arXiv:2412.11006*, 2024b.

- Jianghangfan Zhang, Yibo Yan, Kening Zheng, Xin Zou, Song Dai, and Xuming Hu. Gm-prm: A generative multimodal process reward model for multimodal mathematical reasoning. *arXiv preprint arXiv:2508.04088*, 2025a.
- Jusheng Zhang, Kaitong Cai, Xiaoyang Guo, Sidi Liu, Qinhan Lv, Ruiqi Chen, Jing Yang, Yijia Fan, Xiaofei Sun, Jian Wang, et al. Mm-cot: a benchmark for probing visual chain-of-thought reasoning in multimodal models. *arXiv preprint arXiv:2512.08228*, 2025b.
- Kaiyan Zhang, Jiayuan Zhang, Haoxin Li, Xuekai Zhu, Ermo Hua, Xingtai Lv, Ning Ding, Biqing Qi, and Bowen Zhou. Openprm: Building open-domain process-based reward models with preference trees. In *The thirteenth international conference on learning representations*, 2025c.
- Lingyin Zhang, Jun Gao, Xiaoxue Ren, and Ziqiang Cao. The bidirectional process reward model. *arXiv preprint arXiv:2508.01682*, 2025d.
- Renrui Zhang, Dongzhi Jiang, Yichi Zhang, Haokun Lin, Ziyu Guo, Pengshuo Qiu, Aojun Zhou, Pan Lu, Kai-Wei Chang, Yu Qiao, et al. Mathverse: Does your multi-modal llm truly see the diagrams in visual math problems? In *European Conference on Computer Vision*, pp. 169–186. Springer, 2024c.
- Zhenru Zhang, Chujie Zheng, Yangzhen Wu, Beichen Zhang, Runji Lin, Bowen Yu, Dayiheng Liu, Jingren Zhou, and Junyang Lin. The lessons of developing process reward models in mathematical reasoning. *arXiv preprint arXiv:2501.07301*, 2025e.
- Jian Zhao, Runze Liu, Kaiyan Zhang, Zhimu Zhou, Junqi Gao, Dong Li, Jiafei Lyu, Zhouyi Qian, Biqing Qi, Xiu Li, et al. Genprm: Scaling test-time compute of process reward models via generative reasoning. *arXiv preprint arXiv:2504.00891*, 2025.
- Congming Zheng, Jiachen Zhu, Zhuoying Ou, Yuxiang Chen, Kangning Zhang, Rong Shan, Zeyu Zheng, Mengyue Yang, Jianghao Lin, Yong Yu, et al. A survey of process reward models: From outcome signals to process supervisions for large language models. *arXiv preprint arXiv:2510.08049*, 2025.
- Jinguo Zhu, Weiyun Wang, Zhe Chen, Zhaoyang Liu, Shenglong Ye, Lixin Gu, Hao Tian, Yuchen Duan, Weijie Su, Jie Shao, et al. Internvl3: Exploring advanced training and test-time recipes for open-source multimodal models. *arXiv preprint arXiv:2504.10479*, 2025.

## 7. Appendix

### A. Structured Visual Constraint Schema

The constraint extractor  $E_\phi$  maps an image-question pair  $(I, q)$  to a structured set  $C = \{c_k\}_{k=1}^K$ . Each  $c_k$  belongs to one of three categories: *numeric*, *relation*, or *structure*. The schema is serialized as a JSON array and is the direct supervision target during SFT (Appendix 7).

#### A.1 Complete Example

The following JSON shows a representative constraint set  $C$  for a geometry problem whose image depicts a combined cone-and-cylinder solid with labeled dimensions.

Example: structured visual constraint set  $C$

```
[
  {
    "category": "numeric",
    "entity": "cylinder base radius",
    "attribute": "length",
    "value": 3,
    "unit": "cm",
```

```

    "confidence": 0.95
  },
  {
    "category": "numeric",
    "entity": "cylinder height",
    "attribute": "length",
    "value": 8,
    "unit": "cm",
    "confidence": 0.92
  },
  {
    "category": "numeric",
    "entity": "cone height",
    "attribute": "length",
    "value": 4,
    "unit": "cm",
    "confidence": 0.88
  },
  {
    "category": "relation",
    "type": "equal",
    "entities": ["cone base radius", "cylinder base radius"],
    "direction": null,
    "confidence": 0.97
  },
  {
    "category": "structure",
    "type": "composite",
    "parts": ["cylinder", "cone"],
    "attachment": ["cone placed on top of cylinder"],
    "adjacency": [],
    "confidence": 0.94
  }
]

```

At test time,  $E_\phi$  predicts  $C$  from  $(I, q)$  directly; no gold constraints are used. During training (Appendix 7), the teacher model provides  $C^*$  as supervision targets.

## A.2 Schema Specification

# B. Checklist–Constraint Matching Function

We describe the type-aware matching function  $m(v_j, C)$  that maps a single checklist claim  $v_j$  to a support score  $p_j \in [0, 1]$ .

## B.1 Claim Parsing

Each checklist item  $v_j$  (produced by the policy’s `visualdependency` field) is a natural-language assertion. We classify it as one of three *claim types*—*numeric*, *relational*, or *structural*—using a lightweight classifier trained on the schema vocabulary. Unclassifiable claims receive a soft fallback score of 0.5 (indicating uncertainty rather than contradiction).

Table 5 | Top-level fields for each constraint category. \* `confidence` is a model-estimated reliability weight in  $[0, 1]$  and is used during matching (Appendix 7).

Category	Key fields	Description
numeric	<code>entity</code> , <code>value</code> , <code>confidence</code> *	<code>attribute</code> , <code>unit</code> ,
relation	<code>type</code> , <code>direction</code> , <code>confidence</code>	<code>entities</code> ,
structure	<code>type</code> , <code>parts</code> , <code>attachment</code> , <code>adjacency</code> , <code>confidence</code>	

## B.2 Type-Specific Matching

**Numeric matching.** For a numeric claim asserting “entity  $e$  has attribute  $a$  equal to value  $x$  (unit  $u$ )”, we search  $C$  for constraints  $c_k$  with matching `entity`  $\approx e$  and `attribute`  $= a$  using token-overlap similarity (Jaccard  $\geq 0.5$ ). Among all matching constraints, we select the one with highest `confidence` and compute

$$p_j^{\text{num}} = \mathbb{1} \left[ \frac{|x - c_k.\text{value}|}{\max(|x|, 1)} < \delta \right] \cdot c_k.\text{confidence}, \quad (16)$$

with tolerance  $\delta = 0.15$ . If no matching constraint exists we set  $p_j^{\text{num}} = 0$ .

**Relation matching.** For a relational claim asserting a `type`  $t$  between entities  $\{e_1, e_2, \dots\}$ , we search  $C$  for constraints with `type`  $= t$  and entity overlap. Entity overlap is measured by set intersection over union (Jaccard) of the entity token sets. We define

$$p_j^{\text{rel}} = \max_{c_k \in C^{(t)}} \text{Jaccard}(\{e_i\}, c_k.\text{entities}) \cdot c_k.\text{confidence}, \quad (17)$$

where  $C^{(t)}$  is the subset of constraints with `type`  $= t$ . Synonym groups are used to handle equivalent relation labels (e.g., `perpendicular`  $\leftrightarrow$  `orthogonal`).

**Structural matching.** For a structural claim specifying a set of parts  $P = \{p_1, \dots, p_m\}$ , we search for composite/graph-type constraints and compute part-list Jaccard similarity:

$$p_j^{\text{str}} = \max_{c_k \in C^{\text{struct}}} \frac{|P \cap c_k.\text{parts}|}{|P \cup c_k.\text{parts}|} \cdot c_k.\text{confidence}. \quad (18)$$

## B.3 Score Aggregation

The per-claim score  $p_j$  is the type-specific score from the matched sub-routine. If no constraint can be matched (empty  $C$  or entirely disjoint entity vocabulary), we apply a *soft fallback*:  $p_j = 0.5$ , reflecting neutral evidence rather than active contradiction.

The per-sample visual reliability score  $r$  (Eq. (6) of the main paper) is the geometric mean of all  $\{p_j\}$ :

$$r = \exp\left(\frac{1}{M} \sum_{j=1}^M \log(\epsilon + p_j)\right), \quad \epsilon = 10^{-6}. \quad (19)$$

The geometric mean is deliberately sensitive to catastrophic failures: if any  $p_j \approx 0$  (a clear contradiction between checklist and evidence), the product collapses and  $r$  is pulled sharply downward regardless of how well other claims are supported. This asymmetry is intentional—a single deeply misperceived premise can invalidate the entire trace, and EVPV’s gating should reflect this.

## C. Training Details

### C.1 Dataset Construction

**Constraint distillation.** We sample 20,000 image–question pairs from VisualPRM400K and annotate each with a gold constraint set  $C^*$  using `qwen3-vl-235b-a22b-instruct` as the teacher model. The teacher is prompted with the schema from Appendix 7 and instructed to output a JSON array of constraints; responses that fail schema validation are filtered. The resulting 20K pairs form the SFT corpus for the constraint extractor  $E_\phi$ .

**Step verifier labels.** We use the process-level correctness annotations from VisualProcessBench (Wang et al., 2025b), which provides  $\{y_t\}$  labels ( $y_t \in \{0, 1\}$ ) for each step in each solution trace. These labels are the direct supervision targets for the step verifier  $V_\theta$ .

### C.2 Constraint Extractor $E_\phi$

**Architecture.**  $E_\phi$  is initialized from a pre-trained multimodal VLM backbone (InternVL2.5-8B) and fine-tuned to generate structured constraint JSON conditioned on  $(I, q)$ .

**SFT stage.** We minimize the next-token prediction loss on the JSON serialization of  $C^*$ :

$$\mathcal{L}_{\text{con}}(\phi) = -\log P_\phi(C^* | I, q).$$

Training uses AdamW with learning rate  $2 \times 10^{-5}$ , linear warmup over the first 3% of steps, cosine decay, batch size 16, and 3 epochs. Maximum sequence length is 4096 tokens.

**DPO stage.** To improve constraint fidelity on hard cases, we apply DPO after SFT. For each training instance, we sample  $n = 4$  candidates  $\{C^{(i)}\}_{i=1}^4 \sim P_\phi(\cdot | I, q)$  and compute a schema-aware distance to  $C^*$ . The distance combines (i) category-wise constraint recall (fraction of gold constraints recovered), (ii) numeric value deviation (Eq. equation 16), and (iii) relation type precision. The sample closest to  $C^*$  becomes the preferred response  $C^+$ ; the most distant becomes the rejected response  $C^-$ . We then apply the standard DPO objective:

$$\mathcal{L}_{\text{DPO}}(\phi) = -\log \sigma(\beta_{\text{dpo}} [\log P_\phi(C^+ | I, q) - \log P_\phi(C^- | I, q)]),$$

with  $\beta_{\text{dpo}} = 0.1$  and preference-pair weight  $\lambda_{\text{dpo}} = 0.1$ . The full extractor objective is  $\mathcal{L}_E(\phi) = \mathcal{L}_{\text{con}}(\phi) + \lambda_{\text{dpo}} \mathcal{L}_{\text{DPO}}(\phi)$ . DPO training runs for 1 epoch with learning rate  $5 \times 10^{-6}$ .

### C.3 Step Verifier $V_\theta$

$V_\theta$  is fine-tuned from the same InternVL2.5-8B backbone using binary cross-entropy on per-step correctness labels from VisualProcessBench:

$$\mathcal{L}_V(\theta) = -\sum_{t=1}^T [y_t \log u_t + (1 - y_t) \log(1 - u_t)],$$

where  $u_t = P_\theta(y_t = 1 | I, q, s_{\leq t})$ . Training uses AdamW with learning rate  $2 \times 10^{-5}$ , batch size 8, 3 epochs, and maximum sequence length 8,192 tokens. *Reliability gating is applied only at inference time* as a calibration layer; the verifier is trained on raw step labels without gating.

## C.4 Reliability Gating Hyperparameters

The gating factor  $\alpha(r) = \sigma(\beta(r - \tau))$  (Eq. (9) of the main paper) is controlled by two hyperparameters.

- $\tau = 0.5$ : reliability threshold below which rewards are attenuated. A claim-set where every claim is half-supported yields  $r \approx 0.5$ , which maps to  $\alpha \approx 0.5$  under our sigmoid.
- $\beta = 10$ : sigmoid sharpness. At  $\beta = 10$  the transition from near-zero attenuation ( $r > 0.7$ ) to near-full attenuation ( $r < 0.3$ ) spans roughly 0.4 units of  $r$ , providing a smooth but decisive gate.

**Sensitivity analysis.** Table 6 reports VisualProcessBench overall Macro-F1 under five choices of  $\tau$  (with  $\beta = 10$  fixed). Performance is relatively stable for  $\tau \in [0.4, 0.6]$ , confirming that the method is not strongly sensitive to this threshold.

Table 6 | VisualProcessBench overall Macro-F1 (%) under varying reliability threshold  $\tau$  ( $\beta = 10$  fixed).

$\tau$	0.3	0.4	<b>0.5</b>	0.6	0.7
Macro-F1	66.91	67.23	<b>67.46</b>	67.18	66.74

## D. Complete Prompt Templates

We provide the verbatim prompts used in each pipeline stage. Placeholders are shown in angle brackets (`{...}`).

### D.1 Stage 1 — Structured Image Description Prompt

Used by both the constraint extractor  $E_\phi$  (generating  $C$ ) and in single-image Step-1 of the EVPV-PRM pipeline to produce a natural-language golden description of the image.

#### Stage 1: Structured image description (SYSTEM + USER)

##### [No system prompt — user turn only]

You are a top-tier image analyst and mathematics education expert. Your task is to create a clear, accurate, and solution-critical description of the image provided alongside a math question.

Focus on analyzing the image and generating a structured natural-language description as if explaining the diagram to a student. Your description must cover the following points in one coherent paragraph:

1. **[What is it?]** One sentence summarizing the image type and topic (e.g., "This is a geometric figure showing a combined cone and cylinder.").
2. **[Key elements and data?]** Identify the main mathematical objects (points, lines, shapes, graphs) and list all directly visible numbers, labels, and symbols.
3. **[Important relationships?]** Describe spatial layouts and geometric relationships that are critical for solving the problem.

Output format: a strict JSON code block. The root object must contain a single key `image_description` whose value is the complete description string. Do NOT add any explanatory text outside the JSON block.

--

Question text:

{question\_text}

Image: [image token]

## D.2 Stage 2 — Visual Checklist Evaluation Prompt

Used to score the policy’s visualdependency checklist against the golden description, producing a  $p\_score \in [0, 1]$ .

### Stage 2: Fair visual checklist audit (USER turn)

```
### Fair Visual Checklist Audit: Penalize Direct Contradictions
```

#### [Role and Task]

You are a fair, objective AI auditor. Your sole task is to compare two description lists about the same image: a "Ground-Truth Checklist" (provably correct) and a "Candidate Checklist" (model-generated visual understanding). Evaluate the factual accuracy of the Candidate Checklist.

#### [Core Evaluation Principle]

"Incomplete" is NOT "incorrect." Only a **direct contradiction** counts as an error. Strictly ignore all omissions and missing details.

#### [Inputs]

1. **[Ground-Truth Checklist]:** Verified-correct factual statements about the image.
2. **[Candidate Checklist]:** Model-generated visual fact statements to be audited.

#### [Output Format]

Output a strict JSON code block with three keys:

- **errors\_and\_hallucinations:** array of objects, each representing a direct contradiction. Each object has fields: `faulty_statement`, `correction_or_reason`, `severity` ("High" | "Low"). Empty array [] if no contradictions found.
- **omissions:** string array. **This field does NOT affect scoring and should almost always be []**.
- **p\_score:** float in [0.0, 1.0] representing the final reliability score.

#### [Scoring Rules]

- Start at 1.0.
- Each **High** severity contradiction: deduct 0.5.
- Each **Low** severity contradiction: deduct 0.2.
- Minimum score: 0.0.

#### [High vs Low Severity]

- **High:** contradicts a primary visual fact (object count, key spatial relationship, presence/absence of a main object).
- **Low:** contradicts a secondary detail (background color, non-critical attribute).

--

#### [Ground-Truth Checklist]:

```
{golden_standard_text}
```

#### [Candidate Checklist]:

```
{checklist_to_review_text}
```

## D.3 Stage 3 — Step Reward Judgment Prompt

Used by the step verifier  $V_\theta$  to judge each reasoning step.

**Stage 3: Step reward judgment (USER turn + image)**

You are a professional expert in mathematical reasoning.  
 You will judge whether the CURRENT solution step is correct given the image and the problem.  
 You MUST output ONLY a JSON integer: 1 or -1.

- 1 means the step is correct.
- -1 means the step is incorrect (contradicts the image/question/ previous steps, or is invalid reasoning).

Important:

- Use the image + question + previous steps as context.
- Judge ONLY the CURRENT step relative to the full solution so far.
- Do NOT output any other text, keys, markdown, or explanation.

Problem:  
 {question\_text}

Image description:  
 {image\_description\_text}

Previous steps:  
 {history\_steps\_text}

CURRENT step to evaluate:  
 {current\_step\_text}

Problem image: [image token]

**D.4 Policy Inference Prompt**

Used to elicit structured, step-by-step solutions with per-step visual dependency annotations from the InternVL2.5 policy. A unique nonce and variant\_id are injected per candidate to promote diversity across the  $N = 8$  samples.

**Policy inference prompt (USER turn + image)**

You are a meticulous and precise AI assistant, an expert in visual mathematical reasoning. Your primary goal is to solve the user's query by providing a detailed, step-by-step thought process.

You MUST provide your entire response in a single, valid JSON code block. Do not include any text, explanations, or markdown formatting outside of the JSON object.

--

### DIVERSITY REQUIREMENTS (VERY IMPORTANT)

- This is reasoning variant #{variant\_id}. Your reasoning path should be meaningfully different from other variants.
- Try a different logical decomposition, use different intermediate variables, or vary the order of non-dependent steps.
- Use this nonce strictly as a randomness anchor for this specific generation: {nonce}

--

### JSON OUTPUT SPECIFICATION (CRITICAL)

Your entire output must conform to this JSON schema:

```

{
  "reasoningprocess": [
    {
      "steptext": "A single, clear step of reasoning...",
      "visualdependency": "A specific, observable fact from
                          the image, or null."
    }
  ],
  "finalanswer": "The final answer."
}

Field-Specific Rules:
1. reasoningprocess (List of Objects):
  • steptext: Each step should represent a single calculation, observation,
    or deduction.
  • visualdependency (String or null): Include a description if the step
    directly reads a value/label from the image. Use null ONLY for purely
    abstract steps. CRITICAL: use the JSON literal null, NEVER an empty
    string "".
2. finalanswer (String): For multiple-choice output the option letter only
  (e.g., "A"); for open-ended output the numerical result only.

--

### USER QUERY
{user_query}

```

## D.5 Step Error Attribution in VisualProcessBench

**Step verifier labels.** We use the process-level correctness annotations from VisualProcessBench (Wang et al., 2025b), which provides  $\{y_t\}$  labels ( $y_t \in \{0, 1\}$ ) for each step in each solution trace. These labels are the direct supervision targets for the step verifier  $V_\theta$ .

**Step-level error-type attribution in VisualProcessBench.** VisualProcessBench already provides step-level correctness labels (+1 = correct, -1 = incorrect) for each solution trace. To understand *why* incorrect steps fail and to support the error-distribution statistics reported in the main paper (e.g., the pie charts), we performed **error-type classification** on all steps that are marked incorrect (-1). The taxonomy is two-level. **Top-level categories:** *Visual Misinterpretation* (misreading or misusing the image), *Logical Error* (invalid deduction or reasoning chain), *Calculation Error* (arithmetic or algebraic mistake), *Knowledge Error* (wrong formula or domain fact), and *Incompleteness* (step is underspecified or missing key detail). *Visual Misinterpretation* is further split into **sub-types:** *Structural Misunderstanding* (wrong spatial or geometric structure), *Value Misreading* (wrong number or measure from the figure), and *Object Misidentification* (wrong object, label, or correspondence).

We used a dedicated prompt (see below) with **Gemini-2.5-Pro** to assign, for each incorrect step, one top-level category and, when the model chose Visual Misinterpretation, one sub-type. The model was given the problem text, the image, the full solution, and the index of the incorrect step. **Human annotators** then reviewed a subset of these model-predicted error-type labels, correcting misclassifications (e.g., a step labeled as Calculation Error but actually due to Value Misreading). Disagreements were resolved by discussion or a third annotator. The human-corrected subset was used to evaluate agreement and to refine the remaining labels where needed. The **statistics** reported in the main paper (e.g., 74% Visual Misinterpretation, 19% Logical Error, 3% Calculation Error, 3% Knowledge Error, 1% Incompleteness; and within Visual Misinterpretation, 56% Structural Misunderstanding, 29% Value Misreading, 15% Object Misidentification) are computed from this final, human-verified error-type distribution over all incorrect steps in VisualProcessBench.

The prompt used for the Gemini-2.5-Pro error-type classification pass is given below. The model outputs a JSON object with the chosen top-level category and, when applicable, the visual sub-type.

**Error-type classification prompt (Gemini-2.5-Pro)**

**Task.** You are an expert in mathematical reasoning and multimodal evaluation. You will be given a math problem, an image, a step-by-step solution, and the **index of one step that is already known to be incorrect**. Your job is to classify the **type of error** that best explains why this step is wrong.

**Top-level error types (choose exactly one):**

- **Visual Misinterpretation** — The step is wrong because it misreads or misuses information from the image (wrong shape, number, label, relation, or structure).
- **Logical Error** — The step is wrong due to invalid deduction, wrong implication, or broken reasoning chain (not primarily a visual or calculation mistake).
- **Calculation Error** — The step applies correct reasoning but contains an arithmetic or algebraic mistake.
- **Knowledge Error** — The step uses a wrong formula, definition, or domain fact.
- **Incompleteness** — The step is underspecified, skips necessary detail, or does not fully justify the conclusion.

If you choose **Visual Misinterpretation**, also choose exactly one **sub-type**:

- **Structural Misunderstanding** — Wrong spatial, geometric, or compositional structure (e.g., misidentified layout or parts).
- **Value Misreading** — Wrong numeric value or measure read from the figure (e.g., misread length, angle, or count).
- **Object Misidentification** — Wrong object, label, or correspondence (e.g., confused two elements or misidentified what a symbol refers to).

**Output format.** Reply with a single JSON object in a code block:

```
{
  "top_level": "Visual Misinterpretation" | "Logical Error" |
    "Calculation Error" | "Knowledge Error" | "Incompleteness",
  "visual_subtype": "Structural Misunderstanding" | "Value Misreading" |
    "Object Misidentification" | null
}
```

Set `visual_subtype` to `null` if `top_level` is not “Visual Misinterpretation”.

**Input.**

Problem: {question\_text}

Image: [image]

Solution steps:

Step 1: ...

Step 2: ...

...

The following step is INCORRECT (index {step\_index}): ...

Classify the error type for this step.

## E. Alternative Score Aggregation Strategies

The main paper (Table 2) uses *Geometric Mean*—the fraction of steps with score  $> 0$ —as the trajectory aggregation function for Best-of- $N$  reranking. Here we report results for all five aggregation strategies implemented in the evaluation pipeline.

1. **Geometric Mean:** maps  $R_t \in \{1, -1\}$  to  $\{1.0, 0.1\}$  and takes the geometric mean, making it sensitive to any single incorrect step.
2. **Correctness Rate** (used in main paper):  $\text{Score}(S) = \frac{1}{T} \sum_t \mathbb{1}[R_t > 0]$ .
3. **Streak Score:** rewards consecutive correct-step runs; score is incremented by the current streak length on each correct step and decremented by 1 on each incorrect step, then normalized.
4. **Weighted Correctness:** later steps receive linearly higher weight. Let  $w_t = t$ ; then  $\text{Score}(S) = \frac{\sum_t w_t R_t - W_{\min}}{W_{\max} - W_{\min}}$  where  $W_{\max/\min}$  are the maximum/minimum achievable weighted sums.

5. **First-Error Position:**  $\text{Score}(S) = i^*/T$  where  $i^*$  is the index of the first step with  $R_t = -1$ ; equals 1.0 if no error occurs.

Tables 7–9 report Pass@1 and BoN@8 accuracy (%) for each strategy across three InternVL2.5 policy scales.  $\Delta_8 = \text{BoN@8} - \text{Pass@1}$ .

Table 7 | Best-of-8 reranking under five aggregation strategies, **InternVL2.5-8B** policy. Pass@1 is the same across strategies; BoN@8 and  $\Delta_8$  vary.

Strategy	MathVista			MathVision			MathVerse-VO			WeMath			LogicVista			Overall		
	P@1	B@8	$\Delta_8$	P@1	B@8	$\Delta_8$	P@1	B@8	$\Delta_8$	P@1	B@8	$\Delta_8$	P@1	B@8	$\Delta_8$	P@1	B@8	$\Delta_8$
Geometric Mean	64.5	76.3	+11.8	17.0	22.1	+5.1	22.8	29.5	+6.7	23.5	37.5	+14.0	36.4	45.3	+8.9	32.8	41.7	+8.9
Correctness Rate	64.5	75.1	+10.6	17.0	21.4	+4.4	22.8	28.9	+6.1	23.5	36.8	+13.3	36.4	44.6	+8.2	32.8	41.0	+8.2
Streak Score	64.5	74.8	+10.3	17.0	21.9	+4.9	22.8	28.6	+5.8	23.5	36.5	+13.0	36.4	44.3	+7.9	32.8	40.7	+7.9
Weighted Correctness	64.5	73.2	+8.7	17.0	20.5	+3.5	22.8	27.4	+4.6	23.5	35.1	+11.6	36.4	43.1	+6.7	32.8	39.5	+6.7
First-Error Position	64.5	75.7	+11.2	17.0	22.0	+5.0	22.8	29.0	+6.2	23.5	37.1	+13.6	36.4	44.9	+8.5	32.8	41.3	+8.5

Table 8 | Best-of-8 reranking under five aggregation strategies, **InternVL2.5-26B** policy.

Strategy	MathVista			MathVision			MathVerse-VO			WeMath			LogicVista			Overall		
	P@1	B@8	$\Delta_8$	P@1	B@8	$\Delta_8$	P@1	B@8	$\Delta_8$	P@1	B@8	$\Delta_8$	P@1	B@8	$\Delta_8$	P@1	B@8	$\Delta_8$
Geometric Mean	68.2	79.6	+11.4	23.4	28.1	+4.7	24.0	32.5	+8.5	30.9	42.1	+11.2	39.6	51.7	+12.1	37.2	46.8	+9.6
Correctness Rate	68.2	78.4	+10.2	23.4	27.5	+4.1	24.0	31.8	+7.8	30.9	41.3	+10.4	39.6	50.9	+11.3	37.2	45.8	+8.6
Streak Score	68.2	78.0	+9.8	23.4	27.2	+3.8	24.0	31.4	+7.4	30.9	41.0	+10.1	39.6	50.5	+10.9	37.2	45.4	+8.2
Weighted Correctness	68.2	76.5	+8.3	23.4	26.0	+2.6	24.0	30.1	+6.1	30.9	39.6	+8.7	39.6	49.1	+9.5	37.2	44.0	+6.8
First-Error Position	68.2	79.0	+10.8	23.4	27.9	+4.5	24.0	32.2	+8.2	30.9	41.7	+10.8	39.6	51.2	+11.6	37.2	46.3	+9.1

Table 9 | Best-of-8 reranking under five aggregation strategies, **InternVL2.5-38B** policy.

Strategy	MathVista			MathVision			MathVerse-VO			WeMath			LogicVista			Overall		
	P@1	B@8	$\Delta_8$	P@1	B@8	$\Delta_8$	P@1	B@8	$\Delta_8$	P@1	B@8	$\Delta_8$	P@1	B@8	$\Delta_8$	P@1	B@8	$\Delta_8$
Geometric Mean	71.9	83.5	+11.6	32.2	37.6	+5.4	36.9	47.7	+10.8	38.3	50.0	+11.7	47.9	58.7	+10.8	45.4	55.2	+9.8
Correctness Rate	71.9	82.3	+10.4	32.2	36.8	+4.6	36.9	46.8	+9.9	38.3	49.1	+10.8	47.9	57.8	+9.9	45.4	54.3	+8.9
Streak Score	71.9	81.9	+10.0	32.2	36.4	+4.2	36.9	46.5	+9.6	38.3	48.8	+10.5	47.9	57.5	+9.6	45.4	54.0	+8.6
Weighted Correctness	71.9	80.4	+8.5	32.2	35.0	+2.8	36.9	45.1	+8.2	38.3	47.4	+9.1	47.9	56.1	+8.2	45.4	52.5	+7.1
First-Error Position	71.9	83.0	+11.1	32.2	37.3	+5.1	36.9	47.3	+10.4	38.3	49.6	+11.3	47.9	58.3	+10.4	45.4	54.7	+9.3

Geometric Mean achieves the best or near-best BoN@8 across all scales and benchmarks, while being the simplest to compute. Weighted Correctness is consistently the most conservative: it penalizes any single incorrect step heavily, which sometimes over-rejects good candidates with one minor error. Correctness Rate and First-Error Position closely track Geometric Mean, confirming that the reranking improvement is robust to the choice of aggregation function.

## F. Complete Ablation Results

Table 10 extends Table 4 of the main paper to include all 27 ablation configurations executed in Exp4. Configurations are organized by the component being varied; the *Full Method* row (EVPV + reliability gating) is repeated at the top for reference. All scores are VisualProcessBench Macro-F1 (%);  $\Delta$  is relative to the full method.

Several additional observations emerge from the full table. First, history length shows a consistent monotonic trend: longer history is better, but the marginal gain diminishes quickly beyond 4 steps, suggesting a memory saturation effect. Second, vision sampling temperature has negligible impact on final accuracy ( $|\Delta| < 0.5$ ), indicating that constraint extraction is robust to moderate temperature variation. Third, parse-failure policy matters modestly ( $|\Delta| \leq 1.78$ ): defaulting to  $-1$  (conservative) slightly outperforms defaulting to  $+1$  or random, consistent with VisualProcessBench’s skew toward incorrect steps at harder positions.

Table 10 | Complete ablation results on VisualProcessBench (Macro-F1, %).  $\Delta$  = variant – Full Method. Best per group **bolded**.

Group	Variant	DynaMath	MMMU	MathVerse	MathVision	WeMath	Overall	$\Delta$
Full Method	Full (EVPV + gating)	69.57	68.86	67.09	65.27	69.11	67.46	+0.00
Evidence type	w/o structured facts (caption-only)	67.75	58.09	63.48	60.68	67.10	63.38	-4.08
	w/o constraints (facts = $\emptyset$ )	66.66	55.80	62.61	59.13	65.81	62.11	-5.35
	w/ shuffled facts (structure corrupted)	62.86	52.57	59.81	58.52	64.77	59.82	-7.64
	w/ noise caption only	64.41	56.22	61.05	59.80	65.33	61.18	-6.28
	Short vision prompt	68.02	66.14	65.73	63.91	67.44	66.05	-1.41
	w/ drop-facts corruption	34.90	34.40	36.29	36.14	35.96	35.77	-31.69
Modality	w/o vision (text-only judge, keep JSON)	58.44	49.44	53.59	54.07	61.02	54.93	-12.53
	w/o vision & w/o JSON (text-only)	54.49	43.93	42.78	50.84	53.78	48.23	-19.23
	w/o vision JSON (keep image)	65.83	62.19	63.72	62.44	66.07	64.14	-3.32
Judge prompt	Lenient judge prefix	66.91	65.28	64.02	62.75	67.09	65.13	-2.33
	No-vision judge prefix	57.22	48.71	52.84	53.30	60.14	54.21	-13.25
	Judge temperature 0.2	68.44	67.50	66.11	64.38	68.22	66.58	-0.88
	Judge temperature 0.5	67.83	66.97	65.44	63.76	67.81	66.02	-1.44
History length	History: none	65.74	63.21	62.80	61.45	65.53	63.49	-3.97
	History: last 1 step	66.88	65.42	64.55	63.02	66.91	65.22	-2.24
	History: last 2 steps	67.51	66.09	65.18	63.74	67.60	65.90	-1.56
	History: last 4 steps	68.31	67.44	65.93	64.56	68.40	66.73	-0.73
	History: last 8 steps	68.94	68.21	66.58	64.97	68.82	67.14	-0.32
Vision temp.	Vision temperature 0.0	68.75	67.91	66.43	64.81	68.51	67.01	-0.45
	Vision temperature 0.5	69.02	68.27	66.76	65.01	68.79	67.18	-0.28
	Vision top-p 0.7	68.83	68.44	66.91	65.10	68.93	67.25	-0.21
Parse-failure	Parse fail $\rightarrow$ +1	67.44	66.31	65.02	63.19	67.25	65.68	-1.78
	Parse fail $\rightarrow$ random	67.89	66.74	65.47	63.67	67.72	66.12	-1.34
	Parse fail $\rightarrow$ -1 (default)	<b>69.57</b>	<b>68.86</b>	<b>67.09</b>	<b>65.27</b>	<b>69.11</b>	<b>67.46</b>	+0.00
Compound	No vision JSON + text-only judge	53.11	42.87	41.64	49.72	52.45	47.07	-20.39
	Caption-only + no image in judge	56.72	47.39	49.81	52.14	57.03	52.49	-14.97
	Shuffled facts + lenient judge	61.45	50.88	57.93	56.71	62.24	57.94	-9.52

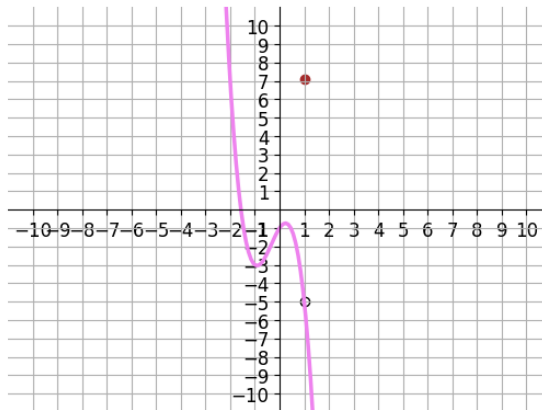
## G. Qualitative Case Studies

We present three cases from VisualProcessBench. In each, **process\_correctness** denotes the *ground-truth* step-level labels (+1 = correct, -1 = incorrect). We show that EVPV-PRM’s step-wise judgments align with (or match) these labels by verifying the policy’s visual claims against extracted constraints  $C$ .

### G.1 DynaMath: Misread kink position

#### Case G.1: Graph — continuous but not differentiable

**Question (DynaMath):** Determine for which values of  $x = a$  the function is continuous but not differentiable at  $x = a$ . Gold answer: 1.



**Extracted constraints  $C$  (by  $E_\phi$ ):**

```

numeric: {entity:"piecewise graph", attribute:"kink position", value:1, unit:"x"}
structure: {type:"graph", parts:["left branch","right branch"],
  attachment:["sharp corner at x = 1"]}
relation: {type:"continuous_at", entities:["function","x=1"], confidence:0.95}
    
```

**Process-level verification.** The policy claims a sharp corner at  $x = -2$  (from step 3 onward);  $C$  gives the kink at  $x = 1$ . Steps 3–6 thus contain an unsupported visual premise. Matching yields low  $p_j$  for those steps; reliability  $r$  is attenuated and step rewards are gated down.

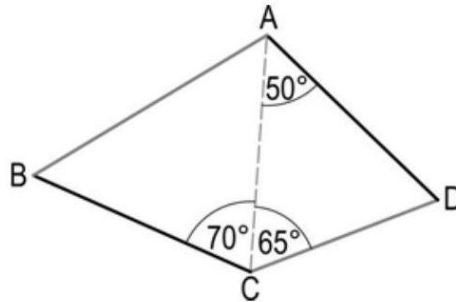
Step (abbreviated)	process_correctness	EVPV step
1 Setup: find where continuous but not differentiable	+1	+1
2 Definitions (continuous / differentiable)	+1	+1
3 “Sharp corner at $x = -2$ ” (visual claim)	-1	-1
4 “Therefore $x = -2$ ” (conclusion)	-1	-1
5 “The answer is $x = -2$ ”	-1	-1
6 Verification of $x = -2$	-1	-1

EVPV-PRM’s step-wise output matches the ground-truth process\_correctness: correct steps 1–2 are preserved; incorrect steps 3–6 are down-weighted because the visual premise contradicts  $C$ .

## G.2 MathVision: Unsupported geometric inference

### Case G.2: Quadrilateral angle (MathVision)

**Question:** In quadrilateral  $ABCD$ ,  $AD = BC$ ,  $\angle DAC = 50^\circ$ ,  $\angle DCA = 65^\circ$ ,  $\angle ACB = 70^\circ$ . How big is  $\angle ABC$ ?  
 Gold answer: B ( $55^\circ$ ).


**Extracted constraints  $C$  (by  $E_\phi$ ):**

```

relation: {type:"equal", entities:["AD","BC"], confidence:0.96}
numeric: {entity:"angle DAC", value:50, unit:"deg"}, ...
structure: {type:"quadrilateral", parts:["A","B","C","D"]}
    
```

**Process-level verification.** Step 1 only restates the problem and figure; its checklist items match  $C$ . Step 2 claims “triangle  $ABC$  is isosceles with  $AB = AC$ ” from  $AD = BC$ ; this claim is not supported by  $C$  (equality is between  $AD$  and  $BC$ , not  $AB$  and  $AC$ ). Steps 2–5 are thus given low reliability and attenuated.

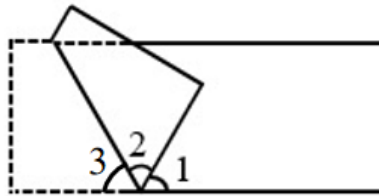
Step (abbreviated)	process_correctness	EVPV step
1 Task and given data ( $AD = BC$ , angles)	+1	+1
2 $\triangle ACD$ : $\angle CAD = 65^\circ$	-1	-1
3 " $AD = BC \Rightarrow AB = AC$ ", $\angle ABC = 70^\circ$	-1	-1
4 Verify angles at C	-1	-1
5 Final answer D ( $70^\circ$ )	-1	-1

Our method's step labels match the ground truth: step 1 is correct and supported by C; steps 2–5 are incorrect and are correctly flagged because the key geometric premise is unsupported.

### G.3 WeMath: Mixed correct/incorrect steps, correct final answer

#### Case G.3: Paper folding (WeMath)

**Question:** When the paper is folded with  $\angle 1 = \angle 2 = \angle 3$ , then  $\angle 1$  equals ( ). A.  $90^\circ$  B.  $45^\circ$  C.  $60^\circ$  D.  $30^\circ$  E. No correct answer. Gold answer: C ( $60^\circ$ ).



**Process-level verification.** The policy infers  $60^\circ$  via “angles form a triangle” and “equilateral” (steps 2–3); the figure does not support that the three angles are interior angles of one triangle. Steps 2–3 are incorrect; steps 4–6 (algebra and final answer) are correct. EVPV assigns low  $p_j$  to the unsupported structural claims in steps 2–3 and preserves reward for steps 4–6.

Step (abbreviated)	process_correctness	EVPV step
1 Key info: $\angle 1 = \angle 2 = \angle 3$	+1	+1
2 “Angles form a triangle; sum $180^\circ$ ”	-1	-1
3 “Equilateral; each $180/3$ ”	-1	-1
4 “Each angle $60^\circ$ ”	+1	+1
5 “Thus $\angle 1 = 60^\circ$ ”	+1	+1
6 Final answer C	+1	+1

EVPV-PRM's step-wise judgment matches process\_correctness exactly: incorrect intermediate reasoning (steps 2–3) is down-weighted; correct conclusion steps (4–6) are preserved, illustrating process-level rather than outcome-only evaluation.